International Journal of Nanomedicine

Dovepress
open access to scientific and medical research

Open Access Full Text Article

ORIGINAL RESEARCH

Aptamer-Targeted Calcium Phosphosilicate Nanoparticles for Effective Imaging of Pancreatic and Prostate Cancer

This article was published in the following Dove Press journal:
International Journal of Nanomedicine

Thomas Abraham[1]
Christopher O McGovern[2]
Samuel S Linton[2]
Zachary Wilczynski[3]
James H Adair[3,4]
Gail L Matters[2]

[1]Departments of Neural and Behavioral Sciences and the Microscopy Imaging Core Facility, The Pennsylvania State University College of Medicine, Hershey, PA, 17033, USA; [2]Department of Biochemistry and Molecular Biology, The Pennsylvania State University College of Medicine, Hershey, PA, 17033, USA; [3]Departments of Materials Science, The Pennsylvania State University, University Park, PA, 16802, USA; [4]Department of Biomedical Engineering and Pharmacology, The Pennsylvania State University, University Park, PA, 16802, USA

Purpose: Accurate tumor identification and staging can be difficult. Aptamer-targeted indocyanine green (ICG)-nanoparticles can enhance near-infrared fluorescent imaging of pancreatic and prostate tumors and could improve early cancer detection. This project explored whether calcium-phosphosilicate nanoparticles, also known as NanoJackets (NJs), that were bioconjugated with a tumor-specific targeting DNA aptamer could improve the non-invasive detection of pancreatic and prostate tumors.

Methods: Using in vivo near-infrared optical imaging and ex vivo fluorescence analysis, DNA aptamer-targeted ICG-loaded NJs were compared to untargeted NJs for detection of tumors.

Results: Nanoparticles were bioconjugated with the DNA aptamer AP1153, which binds to the CCK-B receptor (CCKBR). Aptamer bioconjugated NJs were not significantly increased in size compared with unconjugated nanoparticles. AP1153-ICG-NJ accumulation in orthotopic pancreatic tumors peaked at 18 h post-injection and the ICG signal was cleared by 36 h with no evidence on uptake by non-tumor tissues. Ex vivo tumor imaging confirmed the aptamer-targeted NJs accumulated to higher levels than untargeted NJs, were not taken up by normal pancreas, exited from the tumor vasculature, and were well-dispersed throughout pancreatic and prostate tumors despite extensive fibrosis. Specificity for AP1153-NJ binding to the CCK-B receptor on pancreatic tumor cells was confirmed by pre-treating tumor-bearing mice with the CCK receptor antagonist proglumide. Proglumide pre-treatment reduced the in vivo tumoral accumulation of AP1153-NJs to levels comparable to that of untargeted NJs.

Conclusion: Through specific interactions with CCK-B receptors, tumor-targeted nanoparticles containing either ICG or rhodamine WT were well distributed throughout the matrix of both pancreatic and prostate tumors. Tumor-targeted NJs carrying various imaging agents can enhance tumor detection.

Keywords: tumor detection, ICG nanoparticles, aptamer targeting, proglumide

Introduction

The utility of many conventional tumor imaging agents can be hampered by widespread distribution into unaffected organs or tissues and rapid elimination. Encapsulation of imaging agents into tumor-targeted nanoparticles (NPs) can increase their half-life and enhance the accumulation of imaging agents specifically at the tumor site. However despite these improvements, high interstitial pressure within solid tumors and stromal fibrosis, particularly in pancreatic cancer, often does not permit homogenous distribution of imaging NPs within a tumor.[1] While untargeted NPs can

Correspondence: Gail L Matters
Department of Biochemistry and Molecular Biology, H171, The Pennsylvania State University College of Medicine, PO Box 850, Hershey, PA, 17033, USA
Tel +1 717 531-4098
Fax +1 717 531-7072
Email gmatters@pennstatehealth.psu.edu

submit your manuscript | www.dovepress.com
DovePress
http://doi.org/10.2147/IJN.S295740

passively accumulate in tumors due to the enhanced permeability and retention (EPR) effect, active targeting through the attachment of small molecules such as antibodies, peptides or aptamers to the NP surface can improve the affinity of the NPs for tumor cells and increase NP retention within the tumor microenvironment (TME).

Calcium phosphosilicate NanoJackets (NJs) are a bioresorbable nano-delivery system that is non-toxic, is stable in systemic circulation, and protects encapsulated cargo from metabolic breakdown and clearance.[2–4] These inorganic nanoparticles are resistant to degradation under most physiological conditions yet are designed to release their cargo intracellularly via a pH-dependent disintegration triggered in endosomes.[5,6] However, NJs have no inherent in vivo toxicity. When compared to mice given saline alone, mice injected weekly with NJs demonstrated no significant differences in blood cell counts (WBCs, RBCs, platelets or neutrophils) or serum chemistries (albumin for hepatic function and BUN for renal function) over a four week treatment period.[8] Serum calcium and phosphate levels also were unchanged by NJ treatment, suggesting there was no significant dissolution of the particles in circulation.

CT and/or MRI followed by ultrasound endoscopy based image- guided biopsy is the current standard for cancer early detection of several internal organs, including pancreatic cancer,[10] however detection of pancreatic lesions can be challenging.[11] Patients may undergo optical and/or ultrasound endoscopy based image-guided surgical resection of the tumor or contrast-enhanced ultrasound (CEUS).[12–14] Optical imaging with agents such as the FDA-approved fluorophore indocyanine green (ICG), can be used to improve the contrast between the tumor and the background tissue.[13] Despite the wide use of ICG as a tumor imaging agent, its efficacy is limited by its pharmacokinetic properties - intravenous (i.v.)-injected ICG is rapidly removed from circulation via hepatic clearance with a half-life of approximately 3–4 min.[15] Our research team has demonstrated effective encapsulation of both ICG and rhodamine WT within the matrix of NJs.[8] NJs are optically transparent, do not alter the physical or chemical properties of ICG based on absorption and emission spectra, and stabilize ICG to improve both its half-life and detectable signal depths.[9] The inclusion of polyethylene glycol (PEG) on the particle surface stabilizes NJs, mitigates particle agglomeration and non-specific interactions, and permits attachment of targeting agents. Imaging NJs can be targeted to tumor cells using antibodies, peptides and aptamers. Aptamers are functional nucleic acids with target binding affinity comparable to protein antibodies. Aptamers are more physically and chemically stable, are not immunogenic, and can be produced by standard chemical synthesis with high consistency. Previously, we identified a DNA aptamer (AP1153) which binds to a cell surface G protein coupled receptor, the CCK-B receptor, present on pancreatic tumor cells[16] and prostate tumor cells.[17] A pool of anti-CCKBR DNA aptamers were initially identified using dual SELEX selection with an extracellular, N-terminal portion of the CCKBR (peptide 5–21) as well as selection with a CCKBR over-expressing PANC-1 cell line. Further down-selection of targeting aptamers was based on the predicted secondary structure and receptor binding assays.[16] Here we have shown that through specific interactions with cell surface CCK-B receptors, AP1153 targeted-NJs containing ICG or rhodamine WT were widely distributed throughout tumors and enhanced the detection of pancreatic tumors for up to 24 h after injection.

Materials and Methods

Cultured Cell Lines

PANC-1 human pancreatic cancer cells and PC-3 human prostate cancer cells were cultured in 10% FBS-containing DMEM at 37°C, 5% CO_2. Cells were verified yearly by ATCC STR authentication testing.

Preparation of Imaging Nanoparticles

NanoJackets were prepared by a microemulsion technique that has been previously described.[6] ICG and rhodamine WT encapsulation was accomplished through the addition of the fluorophore into the microemulsion phase such that the fluorescent molecules were trapped and internalized within the particle.[7] After the particles were dissolved to release the dye, fluorophore content was quantified by the optical absorption and compared to a standard curve.

NanoJacket Nanoparticle Characterization

Nanoparticle tracking analysis (NTA) was done using a Nanosight NS300 (Malvern) in a 1X PBS solution. Electron energy loss spectroscopy (EELS) maps were collected on individual particles (n=5 replicates) favorably positioned over a vacuum. The EELS probe was 1 nm in diameter and collected ionization edges every 10 nm across the particle in scanning (STEM) mode. Particle pseudo-coloring and quantification were conducted using Digital MicrographTM software (Gatan Inc., Pleasanton, CA). Transmission electron microscopy (TEM) analysis of rhodamine WT-NJs was done

on a FEI Tecnai G2 Spirit BioTWIN TEM (Materials Characterization Laboratory, The Pennsylvania State University) as previously described.[8] The effects of NanoJackets on in vitro cell growth was determined using an AlamarBlue assay. PC-3 or PANC-1 cells were seeded (7,500 cells/well) into a 96-well plate and grown overnight. After 24 h, cells were transferred into fresh media containing 10% v/v of empty NJs in 1x PBS, 10% v/v of ICG-NJs in 1x PBS, 10% v/v of 1x PBS only (Vehicle), or fresh media alone (Untreated) (n=6 replicates/treatment). Following a 72 h incubation, AlamarBlue reagent was added and the absorbance recorded as per manufacturer's instructions. Cell numbers for all the treatment groups were normalized to the corresponding untreated (media only) cell controls.

Bioconjugation of Aptamer 1153 Onto NanoJackets

A 3′-NH_2-TTTTT version of the CCKBR AP1153 (TriLink, see reference 1 for the complete aptamer sequence) was covalently coupled to carboxy-PEG-NJs using the bioconjugation strategy outlined in Supplemental Figure 1.[18] AP1153 was conjugated to a 2 kDa carboxy-PEG tether on the NJ surface using an EDC/Sulfo-NHS coupling reaction.[8] The resulting AP1153-conjugated NJs were dialyzed to separate unreacted aptamers and sterilized by filtration through a 0.2 mm cellulose membrane.

In vivo Tumor Xenografts

All animal procedures were approved by the Pennsylvania State University College of Medicine Institutional Animal Care and Use Committee (IACUC). The PSU College of Medicine animal resource program is accredited by the Association for Assessment and Accreditation of Laboratory Care International (AAALAC International). All animal living conditions are consistent with standards required by AAALAC International. Four to six week old male athymic (nu/nu) mice were purchased from Charles River. To establish orthotopic pancreatic cancer xenografts, mice were fully anesthetized, a small incision was made in the left flank, the peritoneum was dissected, and the pancreas exposed. Using a 27 gauge needle, $1x10^6$ PANC-1 cells, prepared in 100 µL of Hank's balanced salt solution, were injected into the pancreas and the surgical site closed with staples. All orthotopic tumors were established for 4 weeks prior to imaging. Likewise, subcutaneous PC-3 prostate tumor cells were established by intradermal injection of $1x10^6$ tumor cells and grown for 4 weeks prior to i.v. administration of AP1153-targeted or untargeted ICG-NJs.

In vivo Whole Animal Imaging

NJs were diluted into sterile, phosphate-buffered saline, pH 7.4, and 100 µL was injected via the tail vein into tumor bearing mice. Equivalent ICG or rhodamine WT concentrations were determined prior to injection by absorption spectroscopy. Whole animal imaging was performed as previously described.[6] Near-infrared transillumination images (800 nm excitation, 850 nm emission, 3 min exposure) and corresponding X-ray images were obtained with an in vivo FX whole animal imaging station (Carestream Health, Rochester, NY). ICG signal distribution relative to murine anatomy was illustrated by merging near-infrared and X-ray images.

Ex vivo Tumor Imaging

To assess tumor uptake ex vivo, PANC-1 or PC-3 tumor bearing mice were injected with aptamer-targeted or untargeted NJs loaded with either ICG or rhodamine WT. At 24 h after NJ injection and whole animal imaging but prior to necropsy, mice were injected with tomato lectin-FITC (80 µg/kg, Vector Laboratories) to stain the vascular endothelium. At ten minutes after FITC-lectin injection, mice were quickly perfused with cold PBS/heparin to remove the unbound lectin, and excised tumors were fixed, cryo-protected in 10–30% sucrose, and frozen in OCT. Whole tumors and frozen tumor sections were mounted with ProFade Gold and imaged using Nikon A1 MP+ Multi-Photon Microscope system to assess localization of ICG relative to fibrotic regions of the tumor. Fibrillar collagens indicative of stromal fibrosis were visualized by second harmonic generation (SHG). For 3D image data set acquisition, the multiphoton excitation beam (tuned to 880 nm for SHG and tuned to 820 nm for ICG emission) was first focused at the maximum signal intensity focal position within the tissue sample and the appropriate detector levels (both the gain and offset levels) were then selected to obtain the pixel intensities within the range of 0–4,095 (12-bit images) using a color gradient function. Spectral unmixing was performed to extract the FITC signal from the ICG signal using measured emission spectra. The unmixing algorithm is based on the assumption that the total emission of every channel is expressed as a linear combination of the contributing fluorescence emissions, $I(\lambda)=\Sigma_i C_i \times R_i$. Subsequently, the beginning and end of the 3D stack (ie, the top and the bottom optical sections) were set based on the signal level degradation. For each tissue volume reported here, z-section images

were compiled and the 3D image restoration was performed using IMARIS image analysis software (Bitplane).

Pre-Treatment of Mice with the CCK Receptor Inhibitor Proglumide

One week after tumor cell implantation and three weeks prior to nanoparticle administration, PANC-1 tumor-bearing mice were started on 0.1 mg/mL of the CCK receptor antagonist proglumide ad libitum in drinking water.[19]

Statistical Analyses

Data are presented as mean ± standard error of the mean or mean ± 95% confidence interval as denoted in the figure legends. Comparison of the means between groups was carried out using unpaired two-tailed *t*-tests or one-way ANOVA with Prism 6.0 software (GraphPad), and $p<0.05$ was considered significant.

Results

NanoJacket Characterization

Nanoparticle Tracking Analysis (NTA) was utilized to determine the mean particle diameter of NJs before and after attachment of the 66 nucleotide DNA aptamer AP1153.[16] The size distribution of the NanoJacket populations remained largely the same with or without aptamer bioconjugation (Figure 1A). The overall mean particle diameter was not significantly different between the aptamer targeted and untargeted NJs (Figure 1B). Although some larger particles were detected, the majority of NanoJackets were under 100 nm which is consistent with previous analyses of these particles.[8,9,16] NTA, which was done in a biologically relevant 1X PBS solution that preserves the aptamer structure, demonstrated that aptamer attachment did not precipitate agglomeration or aggregation of these nanoparticles. Electron energy loss spectroscopy (EELS) mapping was done to assess the structural characteristics of NJs. Compositional evaluation of untargeted NJs demonstrated a Ca:P:Si ratio of 1:1.72:0.41 (atomic ratio of 32% Ca, 55% P and 13% Si) (Figure 1C). EELS revealed a homogeneous distribution of components without evidence of architecture that suggested a core or shell enriched in a single element. TEM, which does not visualize bioconjugated aptamers but will reveal the structure and size of the inorganic calcium-phosphosilicate particles, confirmed the spherical form of the NJs and an average particle size of less than 100 nm (Figure 1D). Finally, ICG-NJs had no inherent toxicity towards pancreatic or prostate cancer cells in vitro. After 72 h of incubation in media containing 10%v/v of PBS (Vehicle), 10% v/v of empty NJs in PBS, or 10% v/v of ICG-NJs in PBS, the percentage of viable cells in each treatment group was compared to untreated (media only) control cultures (Figure 1E). For PANC-1 and PC-3 cells, no significant change in cell number was observed for any of the treatment groups in comparison to the untreated control cells.

Aptamer AP1153 Enhances Pancreatic Tumor Uptake of NanoJackets without Accumulation in Non-Tumor, Normal Tissues

Near-infrared (NIR) optical imaging was used to determine the time course of tumor accumulation, biodistribution and clearance of AP1153-targeted versus untargeted ICG-NJs in orthotopic PANC-1 tumor-bearing athymic mice. Sequential NIR whole animal imaging after a single tail vein (i.v.) injection of untargeted ICG-NJs or AP1153-ICG-NJs reveal that the ICG signal was first detected in orthotopic tumors at 12 h post-injection (Figure 2A). Peak uptake of ICG occurred at 18 h after injection with clearance of ICG-NJs by 36–48 h after injection. Whole animal imaging did not reveal any appreciable accumulation of AP1153-ICG-NJs in tissues other than the orthotopic pancreatic tumor. On the whole animal level, untargeted ICG-NJ injected mice showed less detectable ICG signal in tumor tissues than did targeted ICG-NJs (Figure 2A). The timing of nanoparticle uptake by pancreatic tumors was similar to prior reports of untargeted ICG-NJs in vivo, where peak accumulation of the nanoparticles in subcutaneous breast tumors was seen at 24 h after systemic NP administration.[4] At 24 h after i.v. nanoparticle injection, ex vivo near-infrared imaging demonstrated that compared to tumor tissues, adjacent normal pancreas and spleen had little to no uptake of AP1153-ICG-NJs (Figure 2B). Although normal pancreatic acinar cells do express some CCK-B receptors,[20] the AP1153-ICG-NJs do not accumulate to a measurable amount in the normal pancreas.

When other non-tumor tissues were sectioned and examined in greater detail by multi-photon microscopy, AP1153-ICG-NJs were detected circulating in the vasculature of the kidney (Figure 2C), and liver (Figure

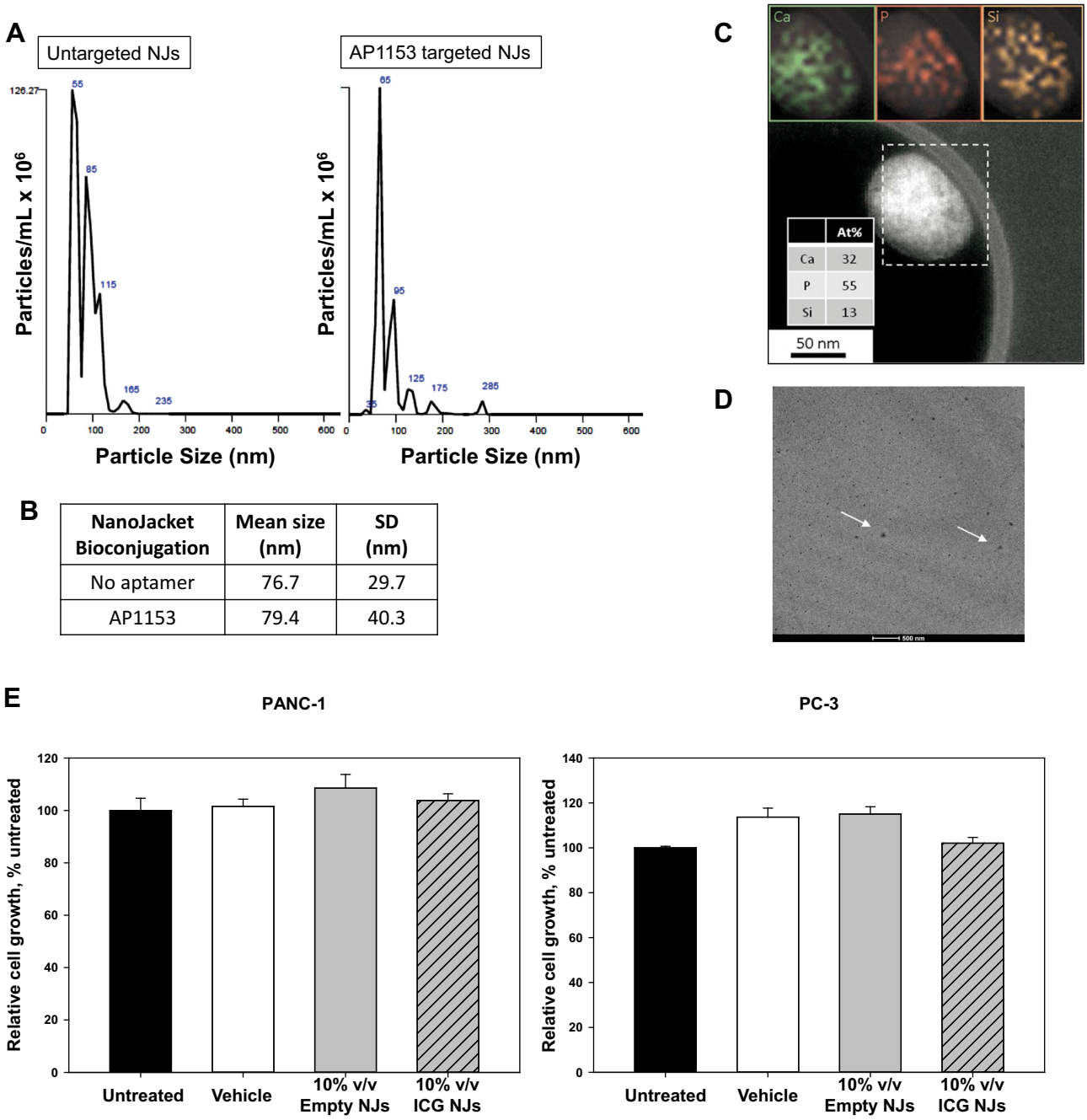

B

NanoJacket Bioconjugation	Mean size (nm)	SD (nm)
No aptamer	76.7	29.7
AP1153	79.4	40.3

Figure 1 NanoJacket characterization. (**A**) Nanosight nanoparticle tracking analysis of untargeted NJs and AP1153-targeted NJs demonstrates that the distribution of nanoparticle sizes, as well as the overall mean diameter of these two groups of nanoparticles (**B**), is not significantly different. Although aptamer AP1153 attachment does slightly increase mean particle diameter, as expected, aptamers do not trigger NJ agglomeration. (**C**) Electron energy loss spectroscopy, EELS, map of elements Ca (green), P (red), and Si (yellow) across a single, representative untargeted NJ. Pseudocoloring of the area indicated by the dashed white line reveals a homogenous distribution of elements throughout the particle with no discernible morphological characteristics, such as a dense particle core or Si rich shell. At% = Ca:P:Si atomic ratio (n=5 replicates), bar scale = 50 nm. (**D**) Transmission electron microscopy of rhodamine WT NJs. White arrows indicate position of representative NJs, scale bar = 500 nm. (**E**) Cell growth studies using PANC-1 and PC-3 cells in vitro demonstrated that even 10% v/v of empty NJs or ICG-loaded NJs had no cellular toxicity (n=6 replicates/cell line, error bars indicate SEM).

2D). This was not unexpected, as nanoparticles are not subject to kidney filtration unless they are <10 nm. In addition, the negative charge of the glomerular basement membrane would likely block the filtration of anionic AP1153-NJs which were previously reported to have a zeta potential of −13 mV in a 70:30 ethanol:water solution.[8] Importantly, there was no evidence of NJ uptake by kidney or liver cells, which was significant

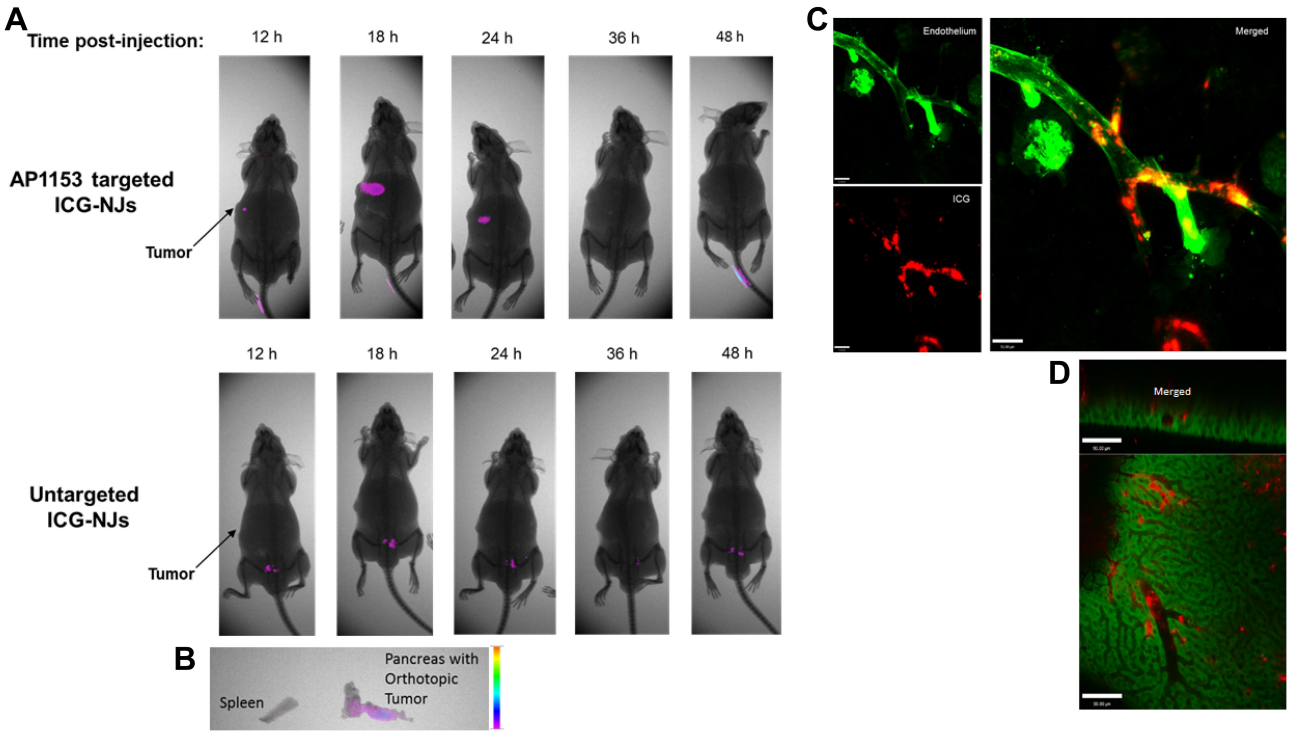

Figure 2 Whole animal and ex vivo NIR optical imaging of targeted AP1153-ICG-NanoJackets in orthotopic pancreatic tumor-bearing mice. (**A**) PANC-1 tumor bearing mice injected with untargeted-ICG-NJs show little tumoral uptake of ICG, while aptamer AP1153-targeted ICG-NJs are well taken up by the orthotopic pancreatic tumor, peak at 18 h post-injection, with no evidence of non-tumoral uptake by normal tissues. Arrows denote the location of orthotopic PANC-1 tumors. (**B**) Ex vivo near-infrared imaging of excised tissues from an AP1153-ICG-NJ treated mouse. Although AP1153-ICG-NJs accumulate in the orthotopic PANC-1 tumor, adjacent normal murine pancreas and spleen had no uptake of AP1153-ICG-NJs. (**C**) Kidney and (**D**) liver tissue sections from an AP1153-ICG-NJ injected mouse showed that although there is some ICG signal (red) within the tissue vasculature (green), no ICG appears to collect inside normal cells within these organs. Size bar for (**D**) = 50 μm, and for (**C**) = 90 μm.

as functional CCKBRs also have been shown to be present on cells of the kidney proximal and distal tubules, collecting ducts and to a lesser extent in glomeruli.[21,22] By 36 to 48 hours after injection, whole animal imaging indicated that AP1153-ICG-NJs were undetectable - suggesting that these particles had either cleared or were degraded and did not build up either within the tumor or in any normal tissues.

AP1153-ICG-NanoJackets Exit the Tumor Vasculature and Accumulate in the Tumor Microenvironment

Although whole animal imaging demonstrated enhanced tumoral uptake of AP1153-ICG-NJs, it did not establish whether the aptamer targeted-ICG-NJs remain in the tumoral vasculature or if the nanoparticles exited the tumor vessels and were distributed throughout the tumor. Tumors excised at 24 h after a single injection of AP1153-ICG-NJs were analyzed ex vivo by multi-photon microscopy. Tumor fibrosis, specifically regions of fibrillar collagen commonly found in desmoplastic pancreatic tumors, was identified by second harmonic generation imaging (SHG). The location of tumor vessels was identified by FITC-lectin endothelial cell stain (Figure 3). Despite the presence of significant fibrosis, the ICG signal from the NanoJackets was detectable throughout the tumor, suggesting that the ICG-NJs were disseminated throughout the tumor matrix (Figure 3A). To establish whether any of the nanoparticles were retained within tumor blood vessels, further imaging of endothelial cell staining relative to the ICG-NanoJacket signal was done. Although the merged image of the endothelial and ICG signals indicated that some of the AP1153-ICG-NJs were associated with the tumor vasculature (yellow on the merged images), most of the ICG signal was found outside of the tumor blood vessels (Figure 3B). This again indicated that the AP1153-ICG-NJs were widely dispersed in the tumor microenvironment regardless of the extensive fibrosis and desmoplasia commonly found in pancreatic tumors.

AP1153 Targeting Enhances the Uptake of ICG-NanoJackets by Subcutaneous PC-3 Prostate Tumors in vivo

Ex vivo imaging of PC-3 prostate tumor cross sections with multiphoton microscopy was used to localize ICG loaded-

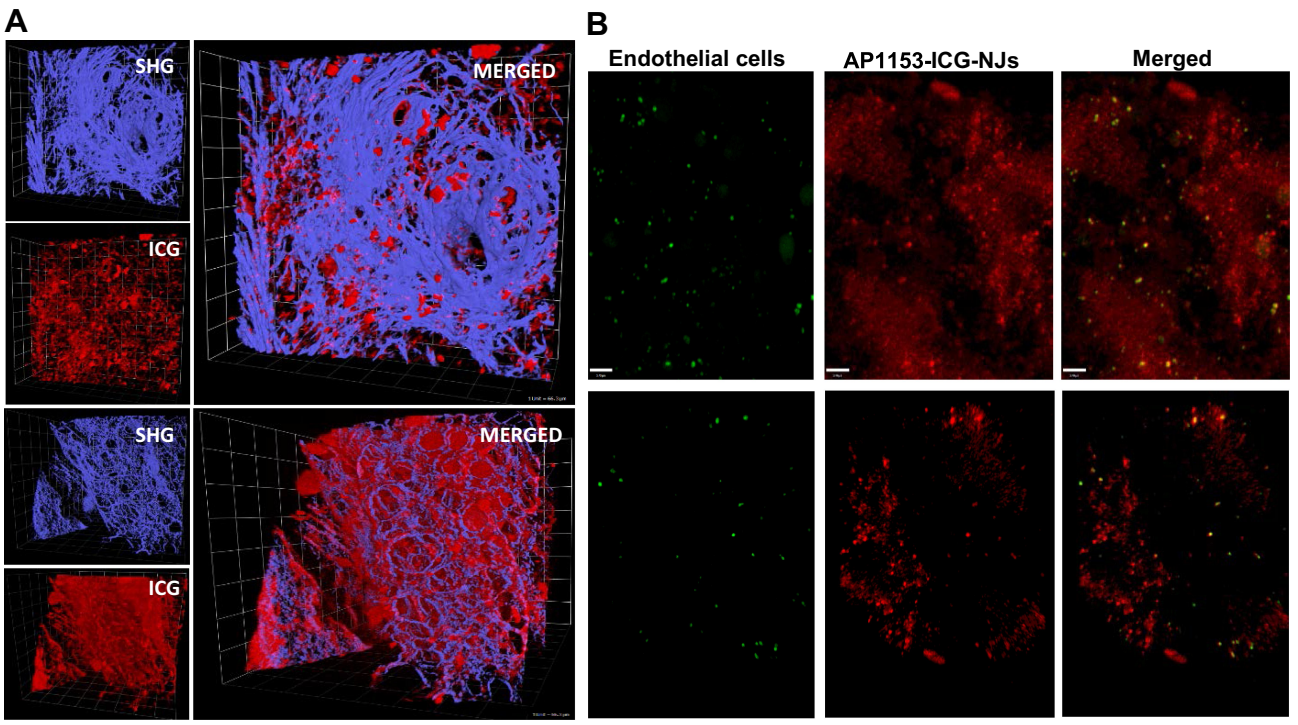

Figure 3 AP1153-ICG-NanoJackets exit the tumor vasculature and are distributed throughout the tumor microenvironment. (**A**) 3D multiphoton images of pancreatic tumor in two independent mice (upper and lower images in both A and B panels) show the spatial distributions of fibrillar collagens (SHG, blue color) and AP1153-ICG nanoparticles (ICG; red color) Box length = 66 μm. (**B**) Compared to the location of tumor vasculature indicated by the endothelial cell stain (green), a majority of the ICG-NJs signal (red) is dispersed outside of the tumor vasculature. Size bar = 5.4 μm.

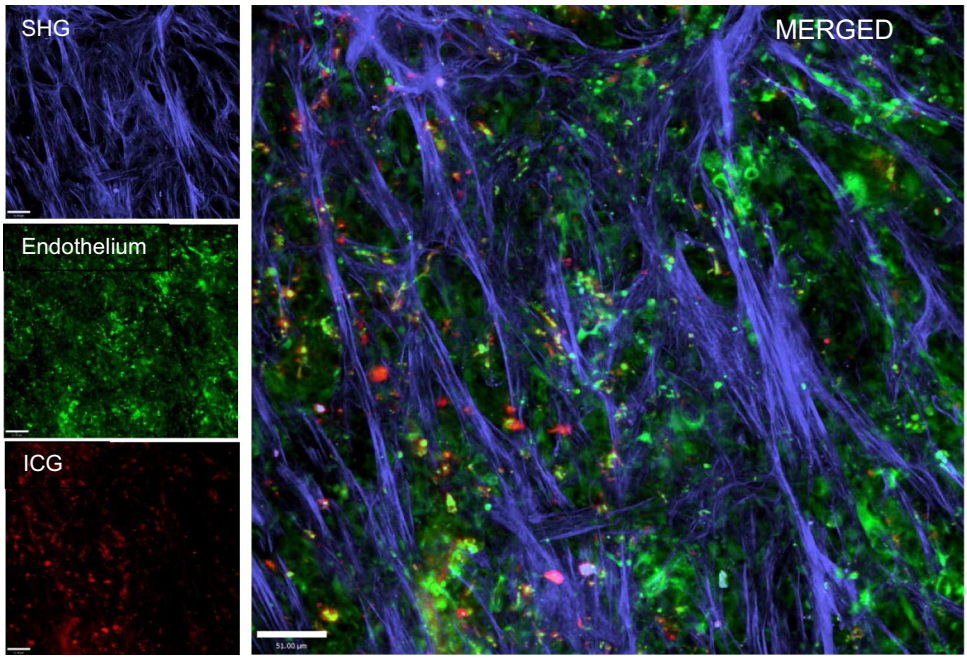

Figure 4 AP1153 targeting enhances the uptake of ICG-NanoJackets by subcutaneous PC-3 prostate tumors in vivo. PC-3 subcutaneous tumor bearing mice were injected with AP1153-ICG-NJs. Using ex vivo multi-photon microscopy, the merged image demonstrates that the AP1153-targeted nanoparticles are primarily outside of the tumor vasculature and are well distributed throughout the tumor. Blue=fibrillar collagen, Green=endothelial cells, Red=ICG, Yellow=merge of ICG with endothelial cells suggesting intravascular or perivascular ICG. White scale bar= 51 μm.

nanoparticles (red) relative to the tumor vasculature (green) and fibrillar collagen regions of the tumor (blue) (Figure 4). Tumors from mice injected with targeted AP1153 conjugated-ICG-NJs showed relatively high ICG signal throughout the tumor. While prostate tumors were less fibrotic and more vascularized than pancreatic tumors (see Figure 3 for comparison), the dispersion of AP1153-ICG-NJs was as widespread in prostate tumors as was seen for pancreatic tumors. Although the majority of ICG is seen in the tumor matrix, yellow signals on the merged image indicated there were some ICG-NJs that remained in the intravascular or perivascular compartments.

AP1153-Targeted NanoJackets Have Increased Accumulation Within Pancreatic Tumors Compared with Untargeted NanoJackets

To further explore the effect of CCKBR aptamer AP1153 targeting on accumulation of imaging nanoparticles within an orthotopic pancreatic tumor, NJs which encapsulated rhodamine WT, rather than ICG, were utilized.[7] As ICG released from nanoparticle encapsulation is rapidly broken down and cleared, these studies utilized the more stable rhodamine WT-NJ formulation to assess the effects of aptamer targeting on the accumulation of imaging agents within the tumors.

Compared with untargeted rhodamine WT-NJs, AP1153 targeted-rhodamine WT-NJs accumulated to a greater extent in orthotopic pancreatic tumors (Figure 5). As seen with the AP1153-ICG-NJs, the AP1153-rhodamine WT-NJs were widely distributed throughout the tumor with some areas of denser NJ accumulation. Although the fluorescent signal in tumor tissue from untargeted-rhodamine WT-NJs injected mice was also well distributed, the overall amount of rhodamine WT nanoparticles accumulating in these tumors was greatly reduced in comparison to the tumoral accumulation of AP1153-rhodamine WT-NJs. This suggested that although there is good dispersion of both the targeted and untargeted NJs within tumors, the overall accumulation of the imaging NJs in pancreatic tumors was enhanced by aptamer AP1153 targeting.

The Accumulation of AP1153-Rhodamine WT-NanoJackets Within Pancreatic Tumors is Reduced After CCK Receptor Blockade

To quantify the amount of AP1153-targeted and untargeted NJs that accumulated in pancreatic tumors, and to verify the role of CCK receptors in AP1153-NJ uptake, three groups of tumor bearing mice were compared. Tumor-bearing animals were injected with AP1153-targeted-rhodamine WT-NJs or untargeted-rhodamine WT-NJs as above while being given normal drinking water. A third group of tumor-bearing mice was pre-treated with the bioavailable, orally administered CCK receptor antagonist proglumide to block these receptors in the tumor prior to AP1153-rhodamine WT-NJ injection. Since AP1153 binds to the extracellular N-terminus of CCK-B receptor, and the antagonist proglumide reversibly binds to the extracellular loops of the CCK-B receptor, blocking its signaling activity,[23] we hypothesized that proglumide would compete with AP1153-rhodamine WT-NJs for binding to the CCK receptors on pancreatic tumor cells in vivo and would reduce tumor-associated rhodamine fluorescence.

When compared to tumors from mice treated with untargeted-rhodamine WT-NJs, tumors from mice injected with AP1153-targeted rhodamine WT-NJs had a significantly higher rhodamine signal (Figure 6, **p= 0.007). Ex vivo imaging of tumors from the proglumide pre-treated animals (+Pro) showed that AP1153-rhodamine WT-NJ uptake was significantly reduced compared with AP1153-rhodamine WT-NJ uptake in tumors from animals given normal drinking water (No Pro; *p=0.015). Quantitatively, proglumide pre-treatment reduced tumoral accumulation of AP1153-rhodamine WT-NJs to a level that was equivalent to that seen in untargeted-NJ injected mice without proglumide pre-treatment. This indicated that while the untargeted NJs entered tumors, the enhanced accumulation of AP1153-rhodamine WT-NJs in pancreatic tumors involved CCK receptors. Although previous in vitro studies demonstrated that the AP1153 aptamer itself bound to PANC-1 cells in a CCK-B receptor mediated fashion,[16] this study confirmed the AP1153-targeted NJs interacted specifically with these receptors in tumors in vivo.

Discussion

The goal of detecting pancreatic cancer early and non-invasively has proven to be difficult. By taking advantage of vascular abnormalities within tumors, such as defective vascular architecture and impaired lymphatic drainage, nanoparticles that are less than 100 nm can accumulate at higher concentrations in tumors than in normal tissues with intact blood vessels.[24] However, the highly fibrotic microenvironment of pancreatic tumors can hinder dispersion of drugs, imaging agents and nanoparticles.[25] The dense tumor stroma,

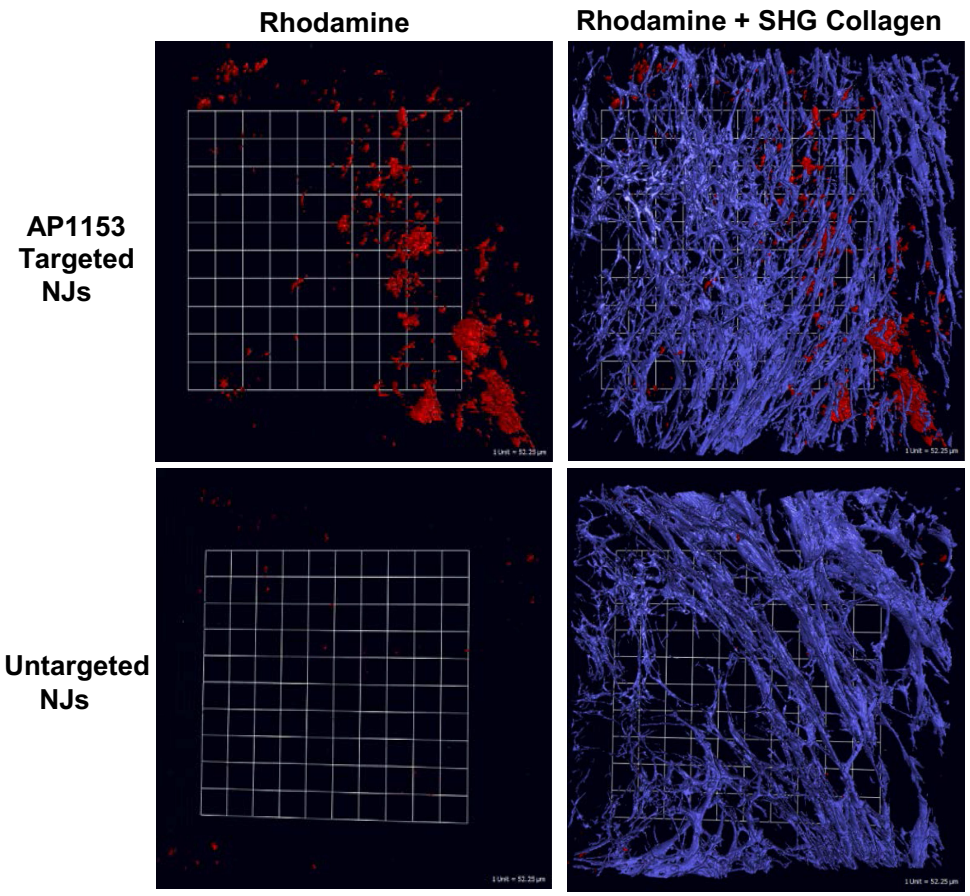

Figure 5 AP1153 targeting enhances nanoparticle accumulation in orthotopic pancreatic tumors. At 24 h after a single tail vein injection of either rhodamine WT-NJs with AP1153 targeting or without AP1153 targeting (Untargeted), tumors were fixed and embedded for fluorescent imaging ex vivo. Significantly more AP1153-ICG-NJs accumulated throughout the orthotopic pancreatic tumors than did untargeted-ICG-NJs. For each image, 1 box length = 52.25 μm. SHG fibrosis images are provided to demonstrate the presence of fibrotic tumor tissue.

with extensive extracellular matrix (ECM) deposition, creates a physical and biochemical barrier to the uptake of imaging agents.[26] Using a murine orthotopic tumor model, which better reflects the tumor microenvironment found in pancreatic cancer patients than do subcutaneous tumors,[27] these studies demonstrate that NJs bioconjugated with the high-affinity, tumor-targeting aptamer AP1153 enhanced the detection of densely fibrotic pancreatic tumors. In addition, size distribution analysis verified that AP1153-conjugation to NJs did not significantly alter the NP size, which was maintained at under 100 nm on average, and did not trigger NP agglomeration. Because the CCK-B receptor is present on the surface of both cancer cells and stellate cells in the tumor microenvironment,[28] the detection efficacy of AP1153-targeted NPs could be greater than for NPs targeted just to tumor cells, as is true for most current tumor imaging strategies.[29]

The relatively short half-life of the NIR imaging agent ICG in vivo is attributed to fluorescence quenching and photo-degradation of free ICG under physiological conditions combined with rapid aggregation and clearance from the body.[15] Previous in vivo studies demonstrated that tumor-associated fluorescence from the untargeted ICG-NJs is significantly prolonged compared to the signal from free ICG.[9] Using whole animal near-infrared imaging, this study demonstrated that encapsulation of ICG into CCK-B receptor-targeted AP1153-NJs further extended its tumoral accumulation in vivo and improved the ICG signal detectable in pancreatic and prostate tumors without off-target, non-specific NP binding.

Previous in vivo studies with AP1153 targeted-ICG-NJs did not discriminate between NPs retained inside the tumor vasculature and those that had exited the tumor vasculature and had accumulated in the tumor matrix. Using both ICG-loaded and rhodamine WT-loaded NJs, we confirmed that not only did the aptamer-targeted nanoparticles leave tumor blood vessels but that they were widely dispersed throughout the tumor. Finally, specificity

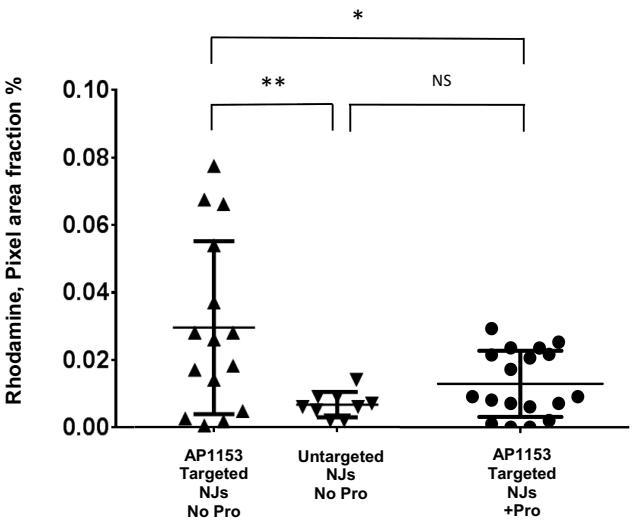

Figure 6 Accumulation of aptamer AP1153 targeted NanoJackets in pancreatic tumors is reduced after CCK receptor blockade. Scatter plot of rhodamine signal in tumors from mice treated with AP1153-targeted or untargeted-rhodamine WT-NJs, as indicated. Tumors from at least 4 mice per treatment group were analyzed ex vivo, and 3–4 images quantified per tumor. No Pro indicates mice that were given only normal drinking water prior to nanoparticle injection; + Pro indicates mice were pre-treated with the CCK receptor antagonist proglumide prior to injection of AP1153-rhodamine WT-NJs. Mean rhodamine signal is indicated by the long horizontal line, while the 95% confidence interval is indicated by the shorter, thicker lines. **p= 0.0070; *p = 0.0155. Tumors from mice pre-treated with a CCK receptor antagonist had significantly less uptake of AP1153-rhodamine WT-NJs than tumors from mice given normal drinking water.
Abbreviation: NS, not significant.

for the AP1153 aptamer targeting to the CCK-B receptor on tumor cells was verified by pre-treating tumor-bearing animals with the CCK receptor antagonist proglumide. Mice pre-treated with proglumide had a significantly less AP1153-rhodamine WT-NJs uptake into their tumors and the amount of targeted nanoparticle uptake in proglumide-treated animals was equivalent to that seen in untargeted nanoparticle-injected mice. Taken together, these data suggested that AP1153-targeted NJs enhance the detection of pancreatic tumors in vivo compared to untargeted nanoparticles specifically through interactions with the CCK-B receptors found on pancreatic and prostate cancer cells.

An advantage of AP1153 as a targeting agent for tumor imaging is the high specificity and affinity that this aptamer has for the CCK-B receptor (15 pM, ~ 3 orders of magnitude better than that of its peptide ligand gastrin).[16] The over-expression of the CCKBR on tumors compared to other adult tissues, and to normal pancreas, also provided specificity for tumor imaging. The whole animal imaging study confirmed that little NIR signal was detected in tissues other than the orthotopic tumors. Although some ICG signal was detected in the vasculature of the liver or kidney, AP1153-targeted-NJs did not accumulate at these sites. Because the highest level of CCKBR expression in non-tumor tissues is in the adult brain, cargo uptake by neural tissues could be a concern. Whole animal NIR imaging demonstrated that there was no evidence of ICG signal in the brain, even up to 48 h after injection, and suggested that AP1153-NJs do not cross the blood-brain barrier.[8] Similarly, the lack of ICG signal outside of the kidney vasculature made AP1153-NJ uptake by CCKBRs present on renal tubular cells unlikely.

The ability to discriminate between normal pancreas and pancreatic tumor tissues in vivo is a key feature if NPs are to be used for early cancer detection. In order to utilize AP1153-ICG-NJs to screen high risk patients for early stage pancreatic cancer, an important distinction is whether normal pancreas accumulates these nanoparticles. AP1153 was selected against a CCK-B receptor peptide epitope with high homology to both human and mouse proteins so it can detect both the human and murine versions of the receptor.[16] Since the ex vivo analysis detected ICG signal in tumor but not in the adjacent normal murine pancreas or spleen, it suggested that these targeted particles could be used for non-invasive pancreatic tumor screening.

Heterogeneity in pancreatic tumor specimens indicates that cancer patients vary widely in terms of their tumor architecture. While some tumors may be highly perfused by abundant leaky vasculature, others exhibit high interstitial fluid pressure, desmoplastic fibrosis, and poor vascular perfusion. Although cancer nanotherapeutics have shown mixed results in clinical trials, nanoparticle-based imaging, using reagents such as the iron-containing nanoparticle ferumoxytol is beginning to be used to assess individual tumor characteristics.[30,31] Ferumoxytol-enhanced magnetic resonance imaging (MRI) enables direct quantitation of tumor vasculature permeability and can define tumor borders to assist in achieving disease-free margin at the time of surgery.[32] Similarly, NIR imaging with AP1153-ICG-NJs could be utilized to identify tumors with higher vessel permeability. Non-invasive imaging with AP1153-ICG-NJS may predict how an individual patient will respond to therapeutics by estimating how much drug is likely to reach the tumor matrix or could be used to stratify treatment decision making.

In the future, one application for AP1153-ICG-NJs could be for sub-tumoricidal photodynamic priming (PDP) prior to administering chemotherapy. Pre-treatment with a NIR-activated PDP agent,

a nanoliposomal benzoporphyrin formulation, followed by nanoliposomal irinotecan was shown to prevent tumor relapse, reduced metastasis and increased survival in a murine pancreatic cancer model.[33] EGFR targeting with a monoclonal antibody (Cetuximab) improved the efficacy of this photosensitizing agent as well.[34] Previous work from our group demonstrated the successful use of untargeted ICG-NJs for photodynamic therapy (PDT) against murine Panc02 tumors in syngeneic C57Bl/6 mice.[35] PDT treatment using ICG-NJs conjugated with CD117-specific antibodies also extended the life span of leukemic mice by targeting leukemia stem cells.[18] The addition of AP1153-targeting to ICG-NJs could enhance the delivery of photosensitizers to pancreatic or prostate tumors. Since other cancers also aberrantly express the CCK-B receptor (lung, gastric),[36] additional studies on AP1153-targeted imaging for early detection or PDT of other tumor types are warranted. Synergistic combinations of receptor-targeted, tumor-specific imaging agents and enhanced detection of NIR signals from AP1153-NJs with photoacoustic devices could advance early detection of pancreatic cancer.[37]

Conclusion

AP1153-NJ imaging nanoparticles incorporate a stable nanoparticle design, effective encapsulation of fluorophore cargoes, and tumor-specific, receptor-mediated targeting to enhance tumor detection. Using whole animal NIR imaging, AP1153-NJs were able to visualize pancreatic tumors, while untargeted-NJs were barely detectable in vivo and demonstrated reduced tumor uptake by ex vivo imaging. Aptamer targeted NJs exited the tumor vasculature in both pancreatic and prostate tumors and the NJs were well dispersed throughout the tumor despite the presence of a highly fibrotic TME. The specificity of aptamer targeting to tumoral CCK receptors in vivo was verified by the reduction in tumor uptake in mice that were pre-treated with the CCKR antagonist proglumide. AP1153-targeted NJ formulations could lead to clinically translatable nanomedicines to provide early cancer diagnosis, guide treatment decision making, or offer a new therapeutic modality.

Abbreviations

AP1153, aptamer 1153; CCKBR, cholecystokinin B receptor; EELS, electron energy loss spectroscopy; EPR, enhanced permeability and retention; FBS, fetal bovine serum; ICG, Indocyanine green; DMEM, Dulbecco's modified Eagle's medium; ECM, extracellular matrix; FITC, fluorescein isothiocyanate; MRI, magnetic resonance imaging; NIR, near-infrared; NJ, NanoJacket; NP, nanoparticle; NTA, Nanoparticle tracking analysis; PDAC, pancreatic ductal adenocarcinoma; PDT, photodynamic therapy; Pro, proglumide; PDP, photodynamic priming; PEG, polyethylene glycol; SHG, second harmonic generation; TME, tumor microenvironment.

Acknowledgments

Penn State Research Foundation has licensed NJ technology to Keystone Nano, Inc. (PA). The support of the Microscopy Imaging Core at Penn State College of Medicine, and the excellent technical assistance of Wade Edris, is gratefully acknowledged. EELS data provided by Dr. Erhan İ. Altınoğlu also is gratefully acknowledged. Samuel S. Linton's present affiliation is at The Rockefeller University, 1230 York Avenue, New York, NY 10065. Zachary Wilczynski's present address is at 224 South Holman Way, Golden, CO 80401, USA.

Funding

This project was supported, in part, by a grant from the Pennsylvania Department of Health using Tobacco CURE Funds to JAH and GLM. GLM also received research funding support from the Penn State Cancer Institute Experimental Therapeutics program and Highmark, Inc. This study was also supported by the NIH grant S100D018124 to TA.

Disclosure

Mr Christopher O McGovern reports a patent "DNA Aptamers Targeting the Cholecystokinin B Receptor (CCKBR) for Diagnosis and Treatment of Pancreatic Ductal Adenocarcinoma and other CCKBR-Expressing Lesions" pending, a patent "Encapsulation and High Loading Efficiency of Phosphorylated Active Prodrug Metabolic Products in Nanoparticles" pending. Dr Samuel S Linton reports a patent PCT/US2017/013769 pending. Dr James H Adair has patents 8,071,132 and 9,145,244 B2 issued to PendreaBio, Inc. JHA is also a cofounder and CSO of Keystone Nano for PendreaBio, Inc. Dr Gail L Matters reports a patent "Encapsulation and High Loading Efficiency of Phosphorylated Active Prodrug Metabolic Products in

Nanoparticles“ pending and a patent “BIOCONJUGATION OF CALCIUMPHOSPHOSILICATE NANOPARTICLES FOR SELECTIVETARGETING OF CELLS IN VIVO” issued. The authors report no other conflicts of interest in this work.

References

1. Tanaka HY, Kano MR. Stromal barriers to nanomedicine penetration in the pancreatic tumor microenvironment. *Cancer Sci*. 2018;109(7):2085–2092. doi:10.1111/cas.13630
2. Adair JH, Parette MP, Altinoglu EI, Kester M. Nanoparticulate alternatives for drug delivery. *ACS Nano*. 2010;4(9):4967–4970. doi:10.1021/nn102324e
3. Altinoglu EI, Adair JH. Near infrared imaging with nanoparticles. *Wiley Interdiscip Rev Nanomed Nanobiotechnol*. 2010;2(5):461–477. doi:10.1002/wnan.77
4. Tabakovic A, Kester M, Adair JH. Calcium phosphate-based composite nanoparticles in bioimaging and therapeutic delivery applications. *Wiley Interdiscip Rev Nanomed Nanobiotechnol*. 2012;4(1):96–112. doi:10.1002/wnan.163
5. Morgan TT, Muddana HS, Altinoglu EI, et al. Encapsulation of organic molecules in calcium phosphate nanocomposite particles for intracellular imaging and drug delivery. *Nano Lett*. 2008;8(12):4108–4115. doi:10.1021/nl8019888
6. Barth BM, Sharma R, Altinoglu EI, et al. Bioconjugation of calcium phosphosilicate composite nanoparticles for selective targeting of human breast and pancreatic cancers in vivo. *ACS Nano*. 2010;4:1279–1287. doi:10.1021/nn901297q
7. Kester M, Heakal Y, Fox T, et al. Calcium phosphate nanocomposite particles for in vitro imaging and encapsulated chemotherapeutic drug delivery to cancer cells. *Nano Lett*. 2008;8(12):4116–4121. doi:10.1021/nl802098g
8. Loc WS, Linton SS, Wilczynski ZR, et al. Effective encapsulation and biological activity of phosphorylated chemotherapeutics in calcium phosphosilicate nanoparticles for the treatment of pancreatic cancer. *Nanomedicine*. 2017;13(7):2313–2324. doi:10.1016/j.nano.2017.06.017
9. Altinoğlu EI, Russin TJ, Kaiser JM, et al. Near-infrared emitting fluorophore-doped calcium phosphate nanoparticles for in vivo imaging of human breast cancer. *ACS Nano*. 2008;2(10):2075–2084. doi:10.1021/nn800448r
10. Yousaf MN, Chaudhary FS, Ehsan A, et al. Endoscopic ultrasound (EUS) and the management of pancreatic cancer. *BMJ Open Gastroenterol*. 2020;7(1):e000408. doi:10.1136/bmjgast-2020-000408
11. Elbanna KY, Jang HJ, Kim TK. Imaging diagnosis and staging of pancreatic ductal adenocarcinoma: a comprehensive review. *Insights Imaging*. 2020;11(1):58. doi:10.1186/s13244-020-00861-y
12. Shirakawa S, Toyama H, Kido M, Fukumoto T. A prospective single-center protocol for using near-infrared fluorescence imaging with indocyanine green during staging laparoscopy to detect small metastasis from pancreatic cancer. *BMC Surg*. 2019;19(1):165. doi:10.1186/s12893-019-0635-0
13. Newton AD, Predina JD, Shin MH, et al. Intraoperative near-infrared imaging can identify neoplasms and aid in real-time margin assessment during pancreatic resection. *Ann Surg*. 2019;270(1):12–20. doi:10.1097/SLA.0000000000003201
14. Ohno E, Kawashima H, Ishikawa T, et al. Can contrast-enhanced harmonic endoscopic ultrasonography accurately diagnose main pancreatic duct involvement in intraductal papillary mucinous neoplasms? *Pancreatology*. 2020;20(5):887–894. doi:10.1016/j.pan.2020.06.004
15. Mordon S, Devoisselle JM, Soulie-Begu S, Desmettre T. Indocyanine green: physicochemical factors affecting its fluorescence in vivo. *Microvasc Res*. 1998;55(2):146–152. doi:10.1006/mvre.1998.2068
16. Clawson GA, Abraham T, Pan W, et al. A cholecystokinin B receptor-specific DNA aptamer for targeting pancreatic ductal adenocarcinoma. *Nucleic Acid Ther*. 2017;27(1):23–35. doi:10.1089/nat.2016.0621
17. Sturzu A, Klose U, Sheikh S, et al. The gastrin/cholecystokinin-B receptor on prostate cells–a novel target for bifunctional prostate cancer imaging. *Eur J Pharm Sci*. 2014;52:69–76. doi:10.1016/j.ejps.2013.10.013
18. Barth BM, Altinoglu E, Shanmugagavelandy SS, et al. Targeted indocyanine-green-loaded calcium phosphosilicate nanoparticles for in vivo photodynamic therapy of leukemia. *ACS Nano*. 2011;5(7):5325–5337. doi:10.1021/nn2005766
19. Smith JP, Cooper TK, McGovern CO, et al. Cholecystokinin receptor antagonist halts progression of pancreatic cancer precursor lesions and fibrosis in mice. *Pancreas*. 2014;43:1050–1059. doi:10.1097/MPA.0000000000000194
20. Rai R, Kim JJ, Tewari M, Shukla HS. Heterogeneous expression of cholecystokinin and gastrin receptor in stomach and pancreatic cancer: an immunohistochemical study. *J Cancer Res Ther*. 2016;12(1):411–416. doi:10.4103/0973-1482.168970
21. Liu T, Jose PA. Gastrin induces sodium-hydrogen exchanger 3 phosphorylation and mTOR activation via a phosphoinositide 3-kinase-/protein kinase C-dependent but AKT-independent pathway in renal proximal tubule cells derived from a normotensive male human. *Endocrinology*. 2013;154(2):865–875. doi:10.1210/en.2012-1813
22. Chen Y, Asico LD, Zheng S, et al. Gastrin and D1 dopamine receptor interact to induce natriuresis and diuresis. *Hypertension*. 2013;62(5):927–933. doi:10.1161/HYPERTENSIONAHA.113.01094
23. Berna MJ, Jensen RT. Role of CCK/gastrin receptors in gastrointestinal/metabolic diseases and results of human studies using gastrin/CCK receptor agonists/antagonists in these diseases. *Curr Top Med Chem*. 2007;7(12):1211–1231. doi:10.2174/156802607780960519
24. Yu M, Zheng J. Clearance pathways and tumor targeting of imaging nanoparticles. *ACS Nano*. 2015;9(7):6655–6674. doi:10.1021/acsnano.5b01320
25. Thomas D, Radhakrishnan P. Tumor-stromal crosstalk in pancreatic cancer and tissue fibrosis. *Mol Cancer*. 2019;18(1):14. doi:10.1186/s12943-018-0927-5
26. Uzunparmak B, Sahin IH. Pancreatic cancer microenvironment: a current dilemma. *Clin Transl Med*. 2019;8(1):2. doi:10.1186/s40169-019-0221-1
27. Miao L, Lin CM, Huang L. Stromal barriers and strategies for the delivery of nanomedicine to desmoplastic tumors. *J Control Release*. 2015;219:192–204. doi:10.1016/j.jconrel.2015.08.017
28. Berna MJ, Seiz O, Nast JF, et al. CCK1 and CCK2 receptors are expressed on pancreatic stellate cells and induce collagen production. *J Biol Chem*. 2010;285(50):38905–38914. doi:10.1074/jbc.M110.125534
29. Nabil G, Bhise K, Sau S, Atef M, El-Banna HA, Iyer AK. Nanoengineered delivery systems for cancer imaging and therapy: recent advances, future directions and patent evaluation. *Drug Discov Today*. 2018;24(2):462–491. doi:10.1016/j.drudis.2018.08.009
30. Miller MA, Arlauckas S, Weissleder R. Prediction of anti-cancer nanotherapy efficacy by imaging. *Nanotheranostics*. 2017;1(3):296–312. doi:10.7150/ntno.20564
31. Siedek F, Muehe AM, Theruvath AJ, et al. Comparison of ferumoxytol- and gadolinium chelate-enhanced MRI for assessment of sarcomas in children and adolescents. *Eur Radiol*. 2020;30(3):1790–1803. doi:10.1007/s00330-019-06569-y

32. Hedgire SS, Mino-Kenudson M, Elmi A, Thayer S, Fernandez-del Castillo C, Harisinghani MG. Enhanced primary tumor delineation in pancreatic adenocarcinoma using ultrasmall super paramagnetic iron oxide nanoparticle-ferumoxytol: an initial experience with histopathologic correlation. *Int J Nanomedicine*. 2014;9:1891–1896. doi:10.2147/IJN.S59788
33. Huang HC, Rizvi I, Liu J, et al. Photodynamic priming mitigates chemotherapeutic selection pressures and improves drug delivery. *Cancer Res*. 2018;78(2):558–571. doi:10.1158/0008-5472.CAN-17-1700
34. Obaid G, Bano S, Mallidi S, et al. Impacting pancreatic cancer therapy in heterotypic in vitro organoids and in vivo tumors with specificity-tuned, NIR-activable photoimmunonanoconjugates: towards conquering desmoplasia? *Nano Lett*. 2019;19(11):7573–7587. doi:10.1021/acs.nanolett.9b00859
35. Barth BM, Shanmugavelandy SS, Kaiser JM, et al. PhotoImmunoNanoTherapy reveals an anticancer role for sphingosine kinase 2 and dihydrosphingosine-1-phosphate. *ACS Nano*. 2013;7(3):2132–2144. doi:10.1021/nn304862b
36. Han Y, Su C, Yu D, et al. Cholecystokinin attenuates radiation-induced lung cancer cell apoptosis by modulating p53 gene transcription. *Am J Transl Res*. 2017;9(2):638–646.
37. Ng TSC, Garlin MA, Weissleder R, Miller MA. Improving nanotherapy delivery and action through image-guided systems pharmacology. *Theranostics*. 2020;10(3):968–997. doi:10.7150/thno.37215